Effect Of DNA-dependent protein kinase on the molecular fate of the rAAV2 genome in skeletal muscle

Sihong Song, Philip J. Laipis, Kenneth I. Berns, and Terence R. Flotte*

Genetics Institute, Powell Gene Therapy Center, Department of Pediatrics, Molecular Genetics, and Microbiology, and Department of Biochemistry and Molecular Biology, University of Florida, Gainesville, FL 32610

Contributed by Kenneth I. Berns, January 9, 2001

We report here that the DNA-dependent protein kinase (DNA-PK) affects the molecular fate of the recombinant adeno-associated virus (rAAV) genome in skeletal muscle. rAAV-human α1-antitrypsin (rAAV-hAAT) vectors were delivered by intramuscular injection to either C57BL/6 (DNA-PKcs$^+$) or C57BL/6-SCID [severe combined immunodeficient (SCID), DNA-PKcs$^-$] mice. In both strains, high levels of transgene expression were sustained for up to 1 year after a single injection. Southern blot analysis showed that rAAV genomes persisted as linear episomes for more than 1 year in SCID mice, whereas only circular episomal forms were observed in the C57BL/6 strain. These results indicate that DNA-PK is involved in the formation of circular rAAV episomes.

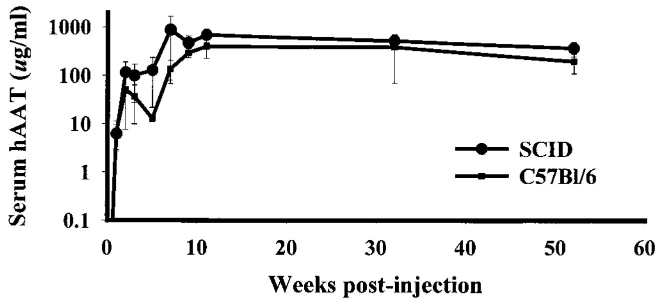

Fig. 1. Long-term transgene expression in murine skeletal muscle transduced with rAAV2. Eight-week-old male C57BL/6 and C57BL/6-SCID mice were injected with 1.4×10^{13} DNA-resistant particles (3.5×10^{10} infectious units) of rAAV-hAAT vector (C-AT). Serum levels of hAAT were measured by ELISA. From week 1 to week 11, each point represents the mean of data from three animals ($n = 3$), and from week 32 to week 52, each point represents data from two animals ($n = 2$).

Recombinant adeno-associated virus (rAAV) vectors have been used increasingly for gene therapy because they are relatively nontoxic and only weakly immunogenic and because the duration of transgene expression with these vectors is prolonged (1, 2). Of the various cells and tissues in which rAAV has been used, skeletal muscle appears to be particularly permissive for efficient and stable expression (3–7). The molecular basis of rAAV persistence in muscle has been examined previously. Integrated and circular episomal forms of rAAV DNA have been found (5, 6, 8). However, long-term persistence of linear episomal forms of rAAV in muscle has not been examined. Furthermore, the effects of host cellular factors on the molecular fate of rAAV are poorly understood.

The DNA-dependent protein kinase (DNA-PK), which is composed of a DNA-binding Ku70/Ku86 heterodimer and a large catalytic subunit (DNA-PKcs), plays an important role in repair of double-stranded DNA breaks and in V(D)J recombination by nonhomologous end-joining (9). It has been reported recently that DNA-PKcs inhibits retrovirus integration (10) and that DNA-PK associated with adenovirus E4 gene products inhibits concatemer formation of adenovirus genome (11). To understand further the molecular fate of the rAAV genome in skeletal muscle and the role of DNA-PK in this process, rAAV-human α1-antitrypsin (rAAV-hAAT) vectors were administered by intramuscular injection into either C57BL/6 (DNA-PKcs$^+$) or C57BL/6-SCID [severe combined immunodeficient (SCID), DNA-PKcs$^-$] mice. These strains differ only at the DNA-PKcs locus. Transgene expression was monitored up to 1 year after injection. Southern blot analysis was used to examine the molecular fate of the vector DNA in each strain.

Materials and Methods

rAAV Vector Preparation and Administration. A single rAAV vector containing both the hAAT coding sequence driven by the cytomegalovirus (CMV) immediate early promoter and the neomycin phosphotransferase (*neo*) gene driven by the herpes simplex virus thymidine kinase (TK) promoter was packaged by using a standard plasmid cotransfection technique followed by iodixanol-gradient purification (7, 12). The physical titer (in DNase-resistant particles) and the biological titer (in infectious units) of each vector preparation was determined by using DNA dot–blot hybridization and the infectious center assay, respectively. Eight-week-old male mice were anesthetized with inhaled metofane. The vector was administered percutaneously by intramuscular injection of a bolus of 1.4×10^{13} DNase-resistant particles split between the right and left quadriceps femoris muscle.

DNA Extraction. Mice were killed at 18, 52, or 78 weeks after injection. The muscle tissue around each injection site was harvested, minced, and incubated in digestion buffer (100 mM NaCl/10 mM Tris·Cl, pH 8/25 mM EDTA, pH 8/0.5% SDS/200 μg/ml proteinase K) with shaking at 50°C overnight. NaCl (5 M) was added to a final concentration of 200 mM. The lysate was extracted twice with buffer-saturated phenol (pH 7.9), twice with phenol/chloroform (50:50), and twice with chloroform followed by ethanol precipitation. To remove the coprecipitated RNA, the DNA solution was incubated with DNase-free RNase at 37°C for 2 h followed by chloroform extraction and ethanol precipitation.

Southern Blot Analysis. Samples of muscle DNA were digested with 100 units each of *Xmn*I, *Hin*dIII, *Bgl*II, or *Sac*I overnight at 37°C, followed by the addition of 10 units of enzyme and incubation at 37°C for 2 additional hours. The activity of each enzyme was checked in a separate reaction, in which plasmid DNA was digested completely. The reactions were stopped by

Abbreviations: rAAV, recombinant adeno-associated virus; DNA-PK, DNA-dependent protein kinase; hAAT, human α1-antitrypsin; SCID, severe combined immunodeficient/immunodeficiency; CMV, cytomegalovirus; MW, molecular weight.

*To whom reprint requests should be addressed. E-mail: flotttr@gtc.ufl.edu.

The publication costs of this article were defrayed in part by page charge payment. This article must therefore be hereby marked "*advertisement*" in accordance with 18 U.S.C. §1734 solely to indicate this fact.

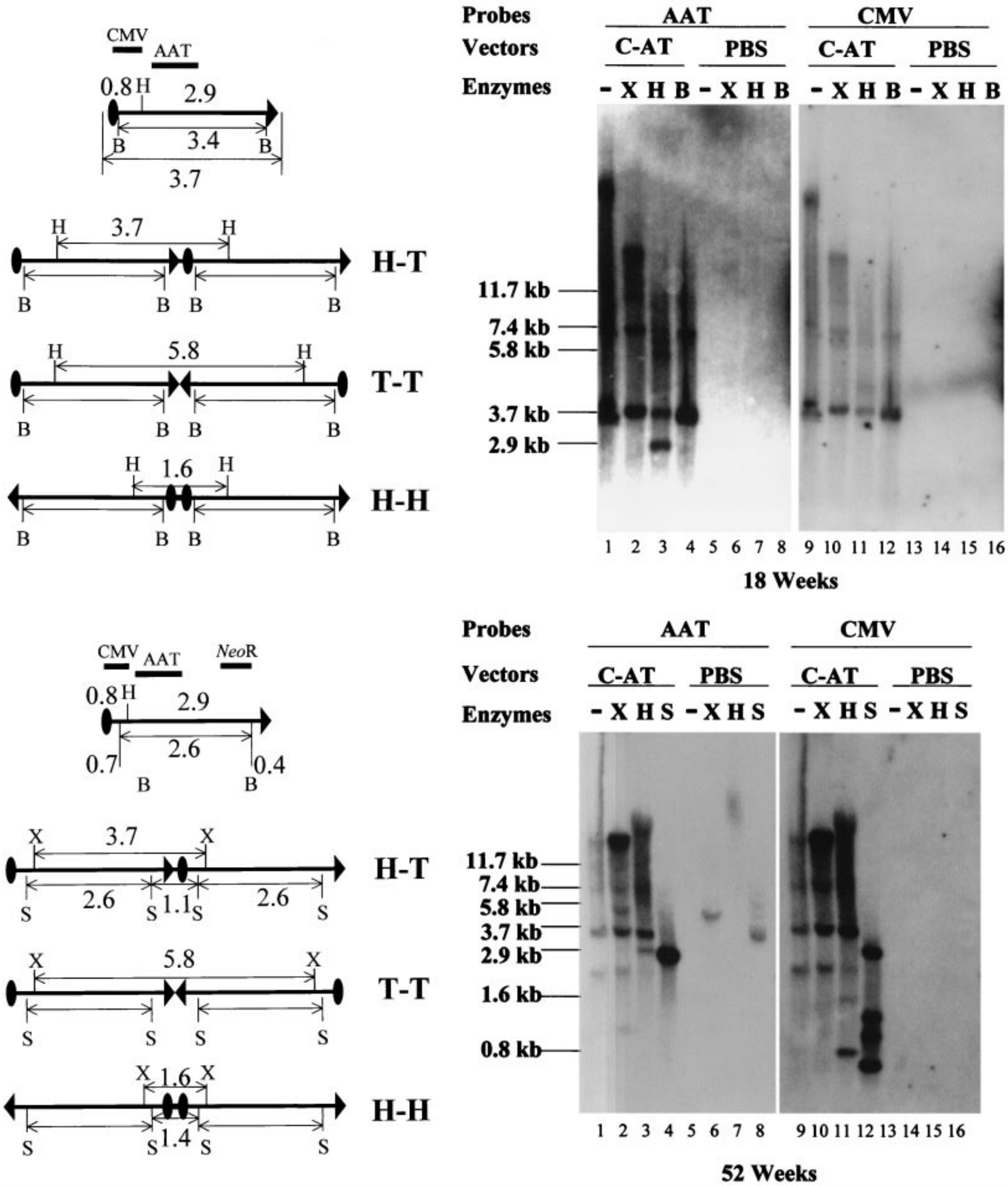

Fig. 2. Linear episomal forms of rAAV2 persist in the skeletal muscle of SCID (DNA-PKcs-deficient) mice. Samples (30 μg/lane) of muscle DNA from vector injection sites were incubated without restriction enzyme (−) or with *Xmn*I (X, no cutting site within the vector), *Hin*dIII (H, cuts the vector once), *Bgl*II (B, cuts the vector twice), or *Sac*I (S, cuts the vector twice). Southern hybridizations were performed with ^{32}P-labeled probes derived from either the hAAT cDNA (AAT) or from the CMV promoter (CMV) as labeled. *A* shows results from the rAAV vector (C-AT)-injected and the PBS-injected SCID mice killed 18 weeks after injection. To the left of the autoradiograph are diagrams of predicted *Hin*dIII (H) and *Bgl*II (B) digestion patterns of the vector DNA in the free ends and all possible junctions, including head-to-head (H-H), tail-to-tail (T-T), and head-to-tail (H-T) junctions. *B* shows the DNA samples (60 μg/lane) from mice killed 52 weeks after injection. To the left of the autoradiograph are diagrams of predicted *Hin*dIII (H) and *Sca*I (S) digestion patterns.

chloroform extraction. DNA was precipitated in ethanol, air-dried, and dissolved in 40 μl of 10 mM Tris/1 mM EDTA, pH 8.0 (TE) before loading on a 0.8% agarose gel. After separation by agarose gel electrophoresis, the DNA fragments were transferred to charged nylon membranes (Immobulon-Ny^{+}; Millipore) by using a rapid downward transfer system (Turboblotter; Schleicher & Schuell). The DNA was cross-linked to the membrane by UV light and baked at 80°C for 2 h. Southern blot hybridization using the appropriate ^{32}P-labeled probe (as indicated in each figure) was performed at 65°C overnight with Church and Gilbert hybridization buffer (0.1% BSA/1 mM EDTA, pH 8.0/250 nM sodium phosphate buffer, pH 7.2/0.7% SDS). Nonspecific binding of probes was eliminated by washing with 40 mM sodium phosphate, pH 7.4/0.75% SDS/1 mM EDTA, pH 8.0 at 65°C. After autoradiography, the radio-labeled probes were stripped by treatment of the membrane with boiled 0.1% SDS. The membrane then was hybridized in an analogous fashion with the next probe (as indicated in each figure).

Densitometric Analysis. The relative densities of each band on the autoradiographic film were measured on a laser densitometer (Ultroscan XL; Pharmacia LKB). The width of the scanning was 1 mm in the center of the lanes. The background signal was estimated by filling a smoothed basal curve and subtracted from the peak area.

Table 1. Relative proportions of rAAV genomes with free tail-ends and with various tail-end junctions in SCID mice

	%	
	18 weeks	52 weeks
Free ends (2.9 kb, from *Hin*dIII)	23.5	1.0
Tail-to-tail (5.8 kb, from *Hin*dIII)*	12.3	2.2
Head-to-tail (3.7 kb, from *Hin*dIII)	18.9	4.5
Vector–cellular genome (deduced)	(45.3)	(92.3)
Total copies of vectors† (internal fragments, from *Bgl*II or *Sca*I)	100	100

*Two copies of vector genomes in each junction.
†The internal fragments were taken as an index of the total copies of rAAV genomes.

Results

The C57BL/6-SCID mouse exhibits SCID on a C57BL/6 genomic background. The nonfunctional immune system of SCID mouse results from a mutation in the DNA-PKcs gene, leading to a defect in V(D)J recombination. This mutation converts the Trp-4046 codon into a stop codon, thus encoding a truncated protein in which the last 83 aa of the kinase domain (13–16) are deleted. Therefore, this animal model can be used as a model for DNA-PKcs deficiency as well as a model of immunodeficiency. In the present study, cohorts of C57BL/6 (n = 3) and C57BL/6-SCID (SCID) mice (n = 3) were injected intramuscularly with 1.4×10^{13} DNase-resistant particles (3.5×10^{10} infectious units) of a rAAV vector (C-AT) expressing hAAT from the CMV immediate early promoter. We have reported previously that these mice expressed and secreted high levels of hAAT into the serum (400–800 μg/ml) for 7–11 weeks after vector injection (7). We now extend these observations for up to 52 weeks postinjection. Surviving animals had serum concentrations of hAAT sustained at levels more than 200–400 μg/ml over the entire time period (Fig. 1).

To determine the molecular fate of the rAAV genome in skeletal muscle, individual mice from each cohort were killed at either 18 weeks or 52 weeks after vector administration. Total cellular DNA from the vector injection site in each animal was isolated and subjected to restriction digestion and Southern blot analysis. The results from the SCID mice killed at 18 weeks are shown in Fig. 2*A*. With undigested DNA, several low-molecular-weight (MW) bands and a smeared high-MW signal were detected by using both the hAAT and the CMV probes (lanes 1 and 9). The low-MW bands were detected more clearly when the DNA was digested with *Xmn*I, which does not cut the vector but does cut the cellular genome (lanes 2 and 10). These low-MW bands matched the predicted sizes of linear monomer (3.7-kb), dimer (7.4-kb), and trimer (11.1-kb) episomal forms of the vector genome. The smeared signal could represent either high-MW episomal concatemers or integrated forms of the vector. However, the migration of this smear was shifted downward when the DNA was digested with *Xmn*I (lanes 2 and 10). This indicated that the smear signal was from vector DNA associated with the host chromosomal DNA and most likely represents integrated forms of the rAAV vector.

Interestingly, when DNA was digested with *Hin*dIII (which asymmetrically cuts the vector genome once), a 2.9-kb band was detected with the hAAT probe (lane 3). As predicted, this 2.9-kb band was not detected with the CMV probe (lane 11), confirming that it represented the free tail-ends of the vector genomes. These free ends can be generated only from linear episomal forms, but not from circular or integrated forms of the vector genome. A 5.8-kb band from the *Hin*dIII digestion also was detected with the hAAT probe (lane 3) and not with the CMV probe (lane 11), indicating that it represented tail-to-tail junctions. Finally, head-to-tail junction fragments of 3.7 kb

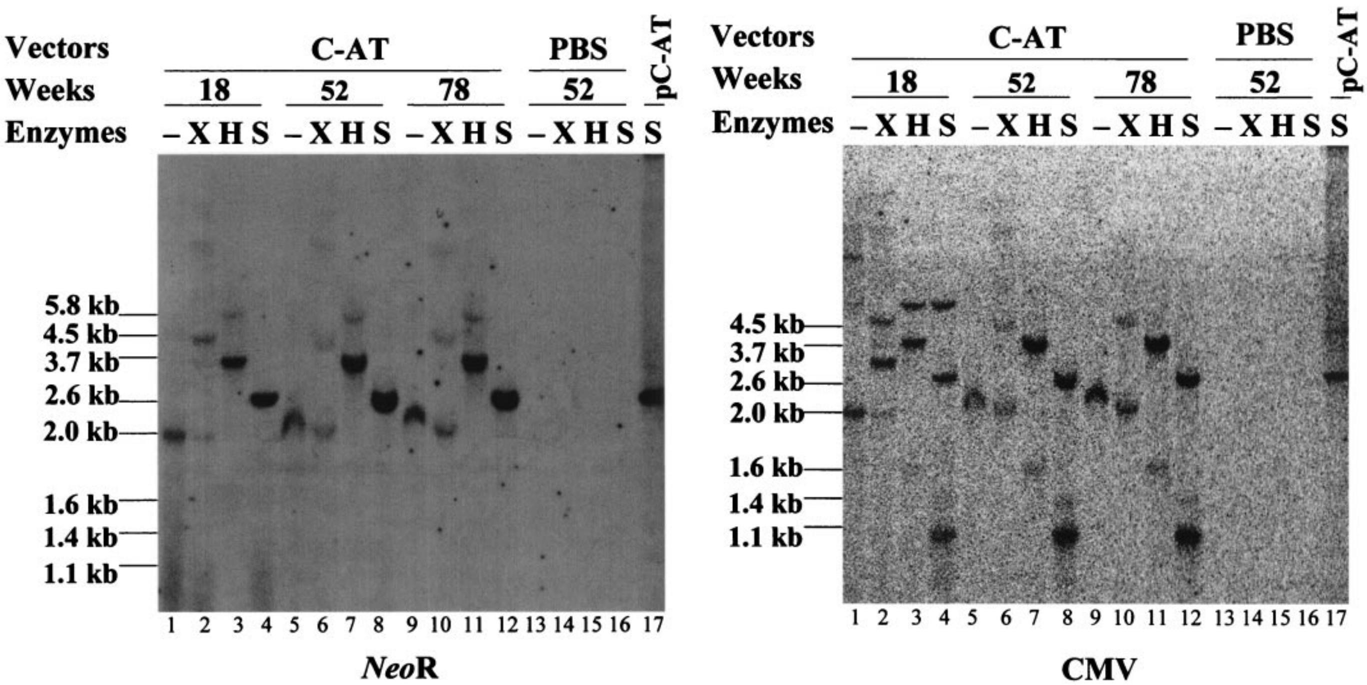

Fig. 3. Circular episomal forms of rAAV persist in the skeletal muscle of C57BL/6 mice. C-AT- or PBS-injected mice were killed 18, 52, and 78 weeks after injection. DNA samples (60 μg/lane) from injection sites were incubated without restriction enzyme (−) or with *Xmn*I (X), *Hin*dIII (H), or *Sac*I (S). Plasmid DNA of C-AT (pC-AT) was digested with *Sac*I to release a 2.6-kb band as a control. (*A*) To avoid the detection of the endogenous murine AAT gene, Southern hybridization was performed with a *neo* cDNA probe (*Neo*R) located downstream of the hAAT gene in the vector (see the diagrams in Fig. 2*B Left*). (*B*) The blot subsequently was stripped and hybridized with the CMV probe.

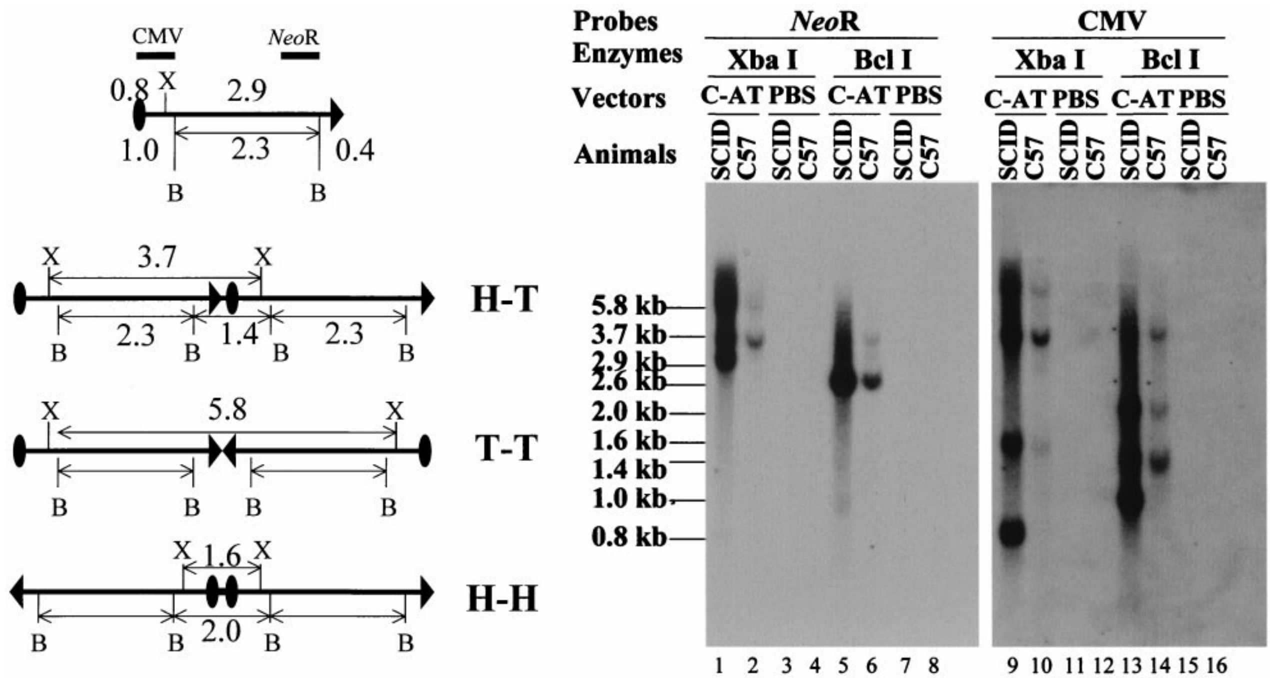

Fig. 4. Detection of episomes in SCID and C57BL/6 mice. To confirm the presence of the free ends in SCID mice and the absence of these ends in C57BL/6 (C57), DNA samples from C-AT- or PBS-injected mice (52 weeks after injection) were digested with *Xba*I (cuts the vector once) or *Bcl*I (cuts the vector twice). Southern blot analyses were performed as described in Fig. 3. To the left of the autoradiograph are diagrams of the predicted *Xba*I (X) and *Bcl*I (B) digestion patterns.

from *Hin*dIII digestion were detected with both probes (lanes 3 and 11).

Digestion of muscle DNA with *Bgl*II (which has two cutting sites within the vector) released a 3.4-kb vector internal vector fragment, which was detectable with the hAAT and the CMV probes (lanes 4 and 12). The intensity of hybridization of this internal fragment represents the total number of copies of rAAV genomes in the sampled tissue. In addition, there was a very faint but detectable band migrating with an apparent size of an 7.4 kb. This apparently incomplete digestion by *Bgl*II could result from DNA methylation or the proximity between the endonuclease recognition sequences and the inverted terminal repeats (ITRs). The *Bgl*II sites could be compromised if the vector DNA was involved in junctions that did not maintain the complete ITR structure (17). Nonetheless, the vast majority of vector genomes are represented within the 3.4-kb *Bgl*II fragment.

To examine the stability of episomal and integrated forms of rAAV, a similar Southern blot analysis was performed on muscle DNA from the SCID mice killed 52 weeks after injection (Fig. 2*B*). Again, in the lanes of unrestricted DNA or DNA cut with *Xmn*I, both episomal and integrated forms were detected with both the hAAT and the CMV probes (lanes 1, 2, 9, and 10). When the DNA was digested with *Hin*dIII, the linear free-tail ends (2.9 kb), the tail-to-tail junctions (5.8 kb), and the head-to-tail junctions (3.7 kb) all were detected with the hAAT probe (lane 3). The linear free-head ends (0.8 kb), the head-to-head junctions (1.6 kb), and the head-to-tail junctions (3.7 kb) all were detected with the CMV probe (lane 11). To avoid the possibility of incomplete digestion, *Sac*I (two cutting sites within the vector) was used to release all of the internal fragments (2.6 kb, lanes 4 and 12). Restriction digestion with *Sac*I also was predicted to release fragments from the linear free-head ends (0.7 kb), head-to-tail junctions (1.1 kb), and head-to-head junctions (1.4 kb). Indeed, all of these were detectable with the CMV probe (lane 12). The detection of free ends from both the tail (2.9 kb) and the head (0.7 and 0.8 kb) of the rAAV vector at 18 weeks and 52 weeks demonstrated the persistence of linear episomal forms of rAAV in skeletal muscle of the DNA-PKcs-deficient mouse.

There were several bands that were detectable in both vector (C-AT)-injected and saline (PBS)-injected mice with the hAAT probe but not with the CMV probe (Fig. 2*B*). The lack of hybridization with the CMV probe indicated that these bands were a result of hybridization of hAAT probe with endogenous murine α1-proteinase inhibitor sequence. These signals were not clearly detectable in Fig. 2*A* because of a difference in the total quantity of DNA loaded per lane. There was also a low-MW signal (migrating at approximately 2 kb) that was observed in the lanes with undigested DNA and *Xmn*III-digested DNA (lanes 1, 2, 9, and 10). This signal was detected with both probes, suggesting that it might represent the supercoiled circular monomer or single-stranded form of the rAAV genome or both. This signal was decreased when the DNA was digested with *Hin*dIII (lanes 3 and 11) and disappeared when the DNA was incubated with *Sac*I (lanes 4 and 12), suggesting that it was mostly from supercoiled circular monomer. It is also possible that positive and negative sense strands annealed during the incubation and subsequently were cleaved at the restriction sites.

We have noted that the relative intensities of the 2.9-kb (free-tail ends) and 3.7-kb (head-to-tail junctions) bands to that of the internal fragment band decreased from 18 weeks to 52 weeks after injection. To more objectively assess the decrease, we used densitometric analysis and estimated the optical density of each tail end and the junction band relative to the internal fragment band (3.4 or 2.6 kb). The relative proportion of vector genomes with free ends (the 2.9-kb fragment) and the proportion involved in vector–vector junctions (the 3.7- and 5.8-kb fragments) decreased, whereas the proportion involved in vector–genome junctions increased from approximately 45% at 18 weeks to approximately 94% at 52 weeks (Table 1). These data suggest that linear episomal forms of the rAAV genome persisted and gradually integrated into the cellular genome.

Surprisingly, similar Southern blot analyses with DNA from C57BL/6 mice (DNA-PKcs $^{+}$) showed a much different molecular fate of rAAV genomes (Fig. 3). First, none of the free-end fragments (0.7, 0.8, or 2.9 kb as detected in the SCID mice) of the vector genome were detected by either hAAT or CMV probes at 18, 52, or 78 weeks after injection. This observation was confirmed further by a side-by-side comparison analysis, in which the free-end fragments (0.8, 1.0, and 2.9 kb) were detected only in the SCID (Fig. 4, lanes 1, 9, and 13) but not in the wild-type C57BL/6 mouse (Fig. 4, lanes 2, 10, and 14). Second, two low-MW bands (4.5 and 2 kb) were detected with unrestricted DNA and DNA cut with *Xmn*I at all times (Fig. 3 *A* and *B*, lanes 1, 2, 5, 6, 9, and 10). The 4.5-kb band, which does not correspond with predicted sizes for linear monomer (3.7 kb) or dimer (7.4 kb), may represent circular episomal forms. The 2-kb band completely disappeared when the DNA digested with *Hin*dIII or *Sac*I (lanes 3, 4, 7, 8, 11, and 12), suggesting that it represents supercoiled circular monomer. Again, head-to-head (1.4- and 1.6-kb), head-to-tail (1.1- and 3.7-kb), and tail-to-tail (5.8-kb) junctions of rAAV genome all were detected (Fig. 3*B*).

Discussion

The contrasting results between C57BL/6 (DNA-PKcs$^+$) and SCID (DNA-PKcs$^-$) mice indicate an important role for DNA-PKcs in determining the molecular fate of the rAAV genome in skeletal muscle. In particular, this protein is involved in recombination between free ends of double-stranded rAAV vector DNA. In the presence of DNA-PK, rAAV DNA forms circular episomes, perhaps by ligation of the blunt, double-stranded ends (18). In the absence of DNA-PK, rAAV DNA remains as a linear monomer or forms linear concatemers. This observation is consistent with and extends the understanding of the functions of DNA-PK in nonhomologous end-joining (9), retrovirus integration (10), and adenovirus concatenation (11). More importantly, this observation provides insight into the involvement of DNA-PK in AAV integration and replication. The data presented here also imply a new molecular mechanism for intermolecular recombination between rAAV genomes, which has been demonstrated recently (19). In SCID mice, the formation of vector–vector junctions indicates that a different cellular pathway may be involved (20). The molecular mechanism underlying the persistence of linear episomes in SCID mice remains to be investigated further. In any case, the elucidation of cellular factors involved in rAAV DNA interactions may be crucial to our understanding of the potential ability of this vector to persist long term in various tissues as well as to our estimates of the potential risk associated with rAAV DNA integration.

This work was supported by grants from Alpha One Foundation and the National Institutes of Health (HL59412, DK51809, HL51811, DK58327, and GM50032). Many thanks to Jianming Wang, Michael Morgan, and the University of Florida Vector Core for technical assistance and rAAV packaging.

1. Flotte, T. R. & Carter, B. J. (1995) *Gene Ther.* **2,** 357–362.
2. Flotte, T. R. & Ferkol, T. W. (1997) *Pediatr. Clin. North Am.* **44,** 153–178.
3. Kessler, P. D., Podsakoff, G. M., Chen, X., McQuiston, S. A., Colosi, P. C., Matelis, L. A., Kurtzman, G. J. & Byrne, B. J. (1996) *Proc. Natl. Acad. Sci. USA* **93,** 14082–14087.
4. Xiao, X., Li, J. & Samulski, R. J. (1996) *J. Virol.* **70,** 8098–8108.
5. Clark, K. R., Sferra, T. J. & Johnson, P. R. (1997) *Hum. Gene Ther.* **8,** 659–669.
6. Snyder, R. O., Spratt, S. K., Lagarde, C., Bohl, D., Kaspar, B., Sloan, B., Cohen, L. K. & Danos, O. (1997) *Hum. Gene Ther.* **8,** 1891–1900.
7. Song, S., Morgan, M., Ellis, T., Poirier, A., Chesnut, K., Wang, J., Brantly, M., Muzyczka, N., Byrne, B. J., Atkinson, M., *et al.* (1998) *Proc. Natl. Acad. Sci. USA* **95,** 14384–14388.
8. Duan, D., Sharma, P., Yang, J., Yue, Y., Dudus, L., Zhang, Y., Fisher, K. J. & Engelhardt, J. F. (1998) *J. Virol.* **72,** 8568–8577.
9. Smith, G. C. & Jackson, S. P. (1999) *Genes Dev.* **13,** 916–934.
10. Daniel, R., Katz, R. A. & Skalka, A. M. (1999) *Science* **284,** 644–647.
11. Boyer, J., Rohleder, K. & Ketner, G. (1999) *Virology* **263,** 307–312.
12. Zolotukhin, S., Byrne, B., Mason, E., Zolotukhin, I., Potter, M., Chesnut, K., Summerford, C., Samulski, R. & Muzyczka, N. (1999) *Gene Ther.* **6,** 973–985.
13. Blunt, T., Gell, D., Fox, M., Taccioli, G. E., Lehmann, A. R., Jackson, S. P. & Jeggo, P. A. (1996) *Proc. Natl. Acad. Sci. USA* **93,** 10285–10290.
14. Danska, J. S., Holland, D. P., Mariathasan, S., Williams, K. M. & Guidos, C. J. (1996) *Mol. Cell. Biol.* **16,** 5507–5517.
15. Araki, R., Fujimori, A., Hamatani, K., Mita, K., Saito, T., Mori, M., Fukumura, R., Morimyo, M., Muto, M., Itoh, M., *et al.* (1997) *Proc. Natl. Acad. Sci. USA* **94,** 2438–2443.
16. Bogue, M. A., Jhappan, C. & Roth, D. B. (1998) *Proc. Natl. Acad. Sci. USA* **95,** 15559–15564.
17. Nakai, H., Iwaki, Y., Kay, M. A. & Couto, L. B. (1999) *J. Virol.* **73,** 5438–5447.
18. Chen, L., Trujillo, K., Sung, P. & Tomkinson, A. E. (2000) *J. Biol. Chem.* **275,** 26196–26205.
19. Nakai, H., Storm, T. A. & Kay, M. A. (2000) *Nat. Biotechnol.* **18,** 527–532.
20. Sanlioglu, S., Benson, P. & Engelhardt, J. F. (2000) *Virology* **268,** 68–78.